MicroRNA-215-5p Promotes Proliferation, Invasion, And Inhibits Apoptosis In Liposarcoma Cells By Targeting MDM2-P53 Signaling Pathways

Zhengnan Song
Tumor Hospital of Xinjiang Medical University
Jingping Bai (vensong@foxmail.com)
Tumor Hospital of Xinjiang Medical University
Renbing Jiang
Tumor Hospital of Xinjiang Medical University
Junshen Wu
Tumor Hospital of Xinjiang Medical University
Wenpeng Yang
Tumor Hospital of Xinjiang Medical University

Research Article

Keywords: Liposarcoma, miR-215-5P, MDM2, Proliferation Invasion Apoptosis

Posted Date: February 21st, 2022

DOI: https://doi.org/10.21203/rs.3.rs-1325504/v1

Abstract

Liposarcoma (LPS) is one of the most common soft tissue malignancies in adults, and LPS is characterized by dysregulation of multiple signaling pathways including MDM2 amplification.MicroRNAs (miRNAs) are involved in tumor progression by regulating gene expression through incomplete complementary pairing with the 3 'untranslated region of mRNAs.In this study, we showed that miR-215-5p could target and promote MDM2 expression, and promote LPS cell proliferation, invasion, and inhibit apoptosis.QRT-PCR showed that the expression of MDM2 was significantly higher when miR-215-5p was overexpressed (2.85 ± 0.48), and dual-luciferase reporter gene showed that the fluorescence intensity ratio decreased in the overexpression group (0.72 ± 0.02), and cell phenotype assay revealed that the proliferation activity increased in the overexpression group, with cell proliferation rates of 104 ± 0.04 (%), 116 ± 0.01 (%), and 120 ± 0.01 (%), increased apoptosis rate (1.47 ± 0.33 (%)), increased colony formation rate (85.10 ± 2.85 (%)), increased cell healing area ratio (30.08 ± 2.00 (%)), and increased cell invasion number (138 ± 3.60) at 24 h, 48 h, and 72 h, respectively; FISH revealed that miR-215-5p colocalized with MDM2, and MDM2 expression increased in the overexpression group, WB suggested that Bax expression decreased, PCNA, Bcl-2, and MDM2 expression increased, and P53 and p21 expression decreased in the overexpression group;These data suggest that miR-215-5p can promote LPS progression through the MDM2-P53 signaling pathway, and targeting miR-215-5p may be a novel therapeutic strategy for the treatment of LPS.

Introduction

Soft tissue malignancies (STS) are defined as a group of malignancies derived from non-epithelial extraosseous tissues, mainly originating from the mesoderm. STS are a highly heterogeneous group of tumors (1). STS accounts for approximately 1% of all malignancies in humans (2), with an annual incidence of approximately 3.4 per 100,000 in the United States (3) and 5 per 100,000 in Europe (4). The incidence of STS has gradually increased in recent years, and the incidence has increased significantly with age (5). With the development of molecular pathology and the application of next-generation sequencing, the histological classification of STS has been revolutionized (6). This poses a challenge to both traditional diagnosis and treatment.

Liposarcoma (LPS) is one of the major types of STS in adults, accounting for approximately 15% – 20% of STS in adults (5). LPS often starts with gradually growing painless, and the prognosis is correlated with the site of growth and the degree of malignancy. The evaluated extended surgical resection can significantly improve the survival of LPS patients within the indications (7) and is the preferred regimen for LPS therapy. LPS are locally aggressive, show infiltrative growth or destructive growth, are prone to local recurrence and distant metastasis, and the 5-year overall survival rate of LPS with regional or distant metastasis is less than 50% (8). LPS mainly includes four subtypes, welldifferentiated (WDL), dedifferentiated (DDL), myxoid (MLS) and pleomorphic (PLS), of which DDL have the highest malignancy with a 10-year survival rate of less than 10% (8).

For the study of LPS genomics, pathogenesis, and signaling pathways, the progress of some novel therapeutic approaches against oncogenic signaling aberrations has been promoted, with *MDM2* (*Murine Double Minute 2*) being the well-studied signaling pathway associated with the progression of LPS. Aberrant amplification of *MDM2* in the genome is present in almost all WDL and DDL (9), and this amplification is considered an important molecular event in the formation of WDL and DDL. Elevated MDM2, as measured by genome amplification and mRNA expression, is associated with a shorter time to relapse (10). It has been confirmed that high *MDM2* copy number is associated with poor prognosis and poor response to cytotoxic drugs (11, 12).

The *MDM2* gene is located on human chromosomes 12q14.3 to q15, with a total length of 491 amino acids, and responds to cellular stress stimuli in a P53-dependent manner, which is involved in cell growth inhibition, apoptosis induction, and cell cycle regulation (13).In normal cells, MDM2 and wild-type P53 regulate each other to form a negative feedback loop. P53 protein can bind to the P2 promoter on *MDM2* and activate *MDM2* expression at the transcriptional level; MDM2 protein binds to key amino acid residues of the N-terminal transactivation domain of P53 and forms a P53-MDM2 complex to inhibit the transcriptional activity of *P53* (14). Second, the MDM2 proteasome itself can act as an E3 ubiquitin ligase that can mediate P53 ubiquitination and degradation, allowing P53 to be maintained at normal physiological low levels (15).MDM2 overexpression can down-regulate P53 activity and promote P53 degradation through the proteasome pathway, which in turn leads to tumor suppressor P53 pathway inactivation, allowing cells to pass through the cell cycle in the presence of DNA damage, which in turn initiates tumorigenesis (16).In addition, MDM2 can regulate cell cycle and apoptosis by interacting with tumor growth suppressors other than P53 (17). *P21* is a downstream gene of *P53*, which encodes a protein that can arrest cell cycle progression and promote apoptosis (18), and MDM2 can promote its degradation by ubiquitinating the marker P21 protein and maintain a low-level state of P21 in the absence of stress signals (19).

MDM2 inhibitors can block the interaction between MDM2 and P53 and upregulate P53 and P21 expression, which in turn inhibits tumor cell proliferation and promotes apoptosis (20). Phase I clinical studies showed that after treatment with MDM2 inhibitor SAR405838 in LPS patients with MDM2 amplification, 71% of patients achieved SD, and in the maximum tolerated dose cohort, 10/18 (56%) achieved SD, with a 3-month progression-free survival (PFR) rate of 32% (21). Showed the importance of MDM2 inhibitors for LPS treatment. In addition, the combination of the MDM2 inhibitor RG7388 and the CDK4/6 inhibitor piperacillin resulted in a significantly longer tumor formation time in mice than either (22). This provides a basis for therapeutic strategies combining targeted inhibition of MDM2 and CDK4/6.

MiRNAs are non-coding RNAs of approximately 19 to 25 nucleotides in length, and miRNAs can pair incompletely with the 3 'untranslated region of target genes (23), which in turn repress target gene expression at the translational level. Recent studies have also shown that miRNAs can promote target gene expression at the transcriptional level by binding to target gene enhancers (24). MiRNAs are involved in the regulation of various intracellular biological processes, and more than one-third of human genes are targeted and regulated by miRNAs. Precise control of miRNA levels is essential for maintaining normal cellular function, while abnormal levels of intracellular miRNAs are closely related to the process of tumorigenesis and progression (25), so miRNAs are promising as predictive biomarkers for the diagnosis, prognosis, and possible therapeutic targets of tumors (26). The target genes and regulatory directions regulated by the same miRNA in different tumor cells may be completely different, for example, miR-215 inhibits cell proliferation by targeted inhibition of stearyl-CoA desaturase (SCD) expression in colorectal cancer (27); while miR-215 inhibits retinoblastoma 1 (RB1) in high-grade gliomas promoting cell proliferation (28).

Taken together, miRNA mediates and participates in the regulation of cell cycle signaling and tumor-related genes and may be a good strategy to explain the mechanism of tumor progression and inhibit tumor cell proliferation and invasiveness. In our study, we selected miR-215-5p, which may target the MDM2 gene, but its mechanism of regulation of MDM2 expression is not clear at present, and there is no evidence to support the role of LPS cell proliferation. The purpose of our study was to investigate the effect of miR-215-5p overexpression and underexpression on MDM2 expression in LPS cells and whether there is a direct regulatory relationship between

the two. We expected to demonstrate the effect of miR-215-5p overexpression and low expression on biological phenotypes such as LPS cell proliferation activity, apoptosis, cell cycle progression, cell invasiveness and metastasis by cell platform. We also expect to confirm the expression changes of caspase-3, MDM2, p53, p21, PCNA, bax, and bcl-2 when miR-215-5p is overexpressed and lowly expressed, as well as to add MDM2 inhibitors to further explore the molecular mechanism of miR-215-5p regulation.

Results

MiRNA and gene selection

We screened differentially expressed mRNA (figure 1A) and miRNA (figure 1B) information between LPS and normal control tissues from the GEO database, and performed GO (supplement 1A) and KEGG (supplement 1B) functional enrichment analysis of differentially expressed genes. We predict all regulatory target genes of differentially expressed miRNAs, and construct mRNA-miRNA regulatory networks (figure 1c) by overlapping genes of differentially expressed miRNA target genes with differentially expressed mRNAs . We applied STRING to construct a differentially expressed protein-protein interaction network and fused it with the mRNA-miRNA regulatory network (figure 1D), and topologically analyzed the fusion network to screen the top 10 key nodes (table 1), which included one miRNA, namely miR-215-5p. For the survival analysis of DDL from the TCGA database (figure 1E), miR-215-5P was suggested to be associated with poor long-term prognosis, although P = 0.08. We used TargetScan to predict miR-215-5P in relation to MDM2 regulation (table 2). Combined with the published literature, we predict that there is a regulatory relationship between miR-215-5p and MDM2 in LPS.

Induction of miR-215-5p expression in LPS cells

The plasmid containing miR-215-5p was transferred into human LPS cells SW-875. Successful transfection was judged by observing miR-215-5p transfection into SW-872 cells. This study showed that after transfection of cells with miR-215-5p mimcs and miR-215-5p inhibitor, green fluorescence appeared (Figure 2A) and transfection was successful. The transfection effect was detected by real-time PCR of transfected cells. The experimental results indicated that the expression of miR-215-5p in the miR-215-5p mimics group was 3.37 ± 0.74, which was significantly increased compared with 1.07 ± 0.22 in the control group, $P < 0.05$ (Figure 2B).

MDM2 expression in LPS cells

Expression of the MDM2 gene was analyzed by qRT-PCR after confirming significant overexpression of miR-215-5p in the transduced cell lines. We analyzed the expression of MDM2 was 2.85 ± 0.48, which was significantly increased compared with 1.00 ± 0.14 in the control group, $P < 0.05$ (Figure 2B).

MiR-215-5p directly regulates MDM2 expression

The relationship between miR-215-5p and the target gene *MDM2* was examined using a dual-luciferase reporter gene. The experimental results showed that co-transfer of miR-215-5p-mimics + wt plasmid resulted in a fluorescence intensity ratio of 0.72 ± 0.02 obtained by Renilla luciferase/firefly luciferase assay, which was significantly lower than the fluorescence intensity ratio of 1.18 ± 0.03 co-transferred with miR-215-5p-mimics NC + wt plasmid, $P < 0.05$. There was no significant difference between the other groups, $P > 0.05$ (Figure 2C).

Mir-215-5p promotes proliferation of SW-872 cells

We investigated the functional effects of miR-215-5 p mimics and inhibitor on SW-872 cells by MTT colorimetric assay. The experimental results revealed that the cell proliferation rates of miR-215-5 p mimics at 24 h, 48 h, and 72 h were 104 ± 0.04 (%), 116 ± 0.01 (%), and 120 ± 0.01 (%), respectively, which were significantly higher than those of the control group (100 ± 0.00 (%), $P < 0.05$; while the cell proliferation rates of miR-215-5 p mimics at 24 h, 48 h, and 72 h were 86 ± 0.01 (%), 81 ± 0.01 (%), and 77 ± 0.01 (%), respectively, which were significantly lower than those of the control group (100 ± 0.00 (%), $P < 0.05$ (Figure 3A).The results confirmed that miR-215-5p significantly promoted cell proliferation.

Mir-215-5p inhibits apoptosis

We analyzed the effects of mir-215-5p on apoptosis and cell cycle in sw-872 cells by flow cytometry. The results showed that the apoptosis rate of miR-215-5p mimics group was 1.47 ± 0.33 (%), which was significantly lower than that of control group (4.89 ± 0.79 (%), $P < 0.05$); the apoptosis rate of miR-215-5p inhibitor group was 24.12 ± 2.20 (%), which was significantly higher than that of control group (4.89 ± 0.79 (%), $P < 0.05$ (Figure 3B).Flow Cytometry for the Detection of Apoptosis Original Figure 3D.

Mir-215-5p promotes cell cycle progression

The cell cycle of the miR-215-5p mimics group was 51.79 ± 2.05 (%) in G1 phase, which was significantly lower than 62.65 ± 3.12 (%) in the control group, $P < 0.05$; 33.54 ± 3.10 (%) in S phase was significantly higher than 26.75 ± 1.12 (%) in the control group, which did not change significantly in G2 phase, $P > 0.05$. The cell cycle of the miR-215-5p inhibitor group was 38.57 ± 1.82 (%) in G1 phase, which was significantly lower than 62.65 ± 3.12 (%) in the control group, $P < 0.05$; there was no significant difference in S phase, $P > 0.05$; and 32.74 ± 1.62 (%) in G2 phase was significantly higher than 10.61 ± 2.09 (%) in the control group, $P < 0.05$ (Figure 3C).Flow Cytometry Detects Cell Cycle Original Figure 3E.

Mir-215-5p promotes invasion and metastasis of SW-872 cells

We investigated the effects of miR-215-5p mimics and inhibitor on the invasion and healing ability of SW-872 cells by cell scratch and invasion assays. The experimental results revealed that the cell healing area ratio of the miR-215-5p mimics group was 30.08 ± 2.00 (%), which was significantly higher than that of the control group 20.86 ± 3.77 (%), $P < 0.05$; the cell healing area ratio of the miR-215-5p inhibitor group was 7.12 ± 2.5 (%), which was significantly lower than that of the control group 20.86 ± 3.77 (%), $P < 0.05$ (Figure 4A).

The original figure is Figure 4d.The number of cell invasion in the miR-215-5p mimics group was 138 ± 3.60, which was significantly increased compared with 97.33 ± 5.51 in the control group, $P < 0.05$; the number of cell invasion in the miR-215-5p inhibitor group was 62 ± 5.57, which was significantly decreased compared with 97.33 ± 5.51 in the control group, $P < 0.05$ (Figure 4B). The original figure is Figure 4E.

Colony formation in the miR-215-5p mimics group was 85.10 ± 2.85 (%), which was significantly higher than that in the control group (67.33 ± 0.58 (%), $P < 0.05$; colony formation in the miR-215-5p inhibitor group was 54.57 ± 3.01 (%), which was significantly lower than that in the control group (67.33 ± 0.58 (%), $P < 0.05$ (Figure 4C).These data suggest that miR-215-5p can intervene in the invasion and metastasis function of SW-872 cells. The original figure is Figure 4F.

MiR-215-5p colocalizes with *MDM2*

We found that miR-215-5p co-localized with *MDM2* by FISH assay (Figure 5A). The expression level of *MDM2* in miR-215-5p mimics group was 0.02 ± 0.002, which was significantly higher than that of the control group (0.006 ± 0.0007), P < 0.05(Figure 5C); the expression level of *MDM2* in miR-215-5p inhibitor group was 0.002 ± 0.0005, which was significantly lower than that of the control group (0.006 ± 0.0007), P < 0.05 (Figure 5D).

Mir-215-5p promotes cell proliferation and inhibits apoptosis

We found by Western blot experiments that the expression of PCNA in the miR-215-5p overexpression group was 0.672 ± 0.08, which was significantly higher than that in the control group 0.44 ± 0.13, P < 0.05; the expression of PCNA after inhibition of miR-215-5p was 0.32 ± 0.15, which was not significantly different from that in the control group 0.44 ± 0.13, P > 0.05. At the same time, the expression of Bcl-2 by miR-215-5p overexpression was 0.69 ± 0.05, which was significantly increased compared with 0.44 ± 0.05 in the control group, P < 0.05; the expression of Bax was 0.27 ± 0.06, which was significantly decreased compared with 0.43 ± 0.07 in the control group, P < 0.05; and the expression of caspase-3 was 0.05 ± 0.02, which was not significantly different from 0.08 ± 0.03 in the control group, P > 0.05.

After inhibition of miR-215-5p, the expression of Bcl-2 was 0.24 ± 0.02, which was significantly lower than 0.44 ± 0.05 in the control group, P < 0.05; the expression of Bax was 0.63 ± 0.08, which was significantly higher than 0.43 ± 0.07 in the control group, P < 0.05; and the expression of caspase-3 was 0.18 ± 0.04, which was significantly higher than 0.08 ± 0.03 in the control group, P < 0.05 (Figure 5H). The original figure is Figure 5E.These data suggest that miR-215-5p plays a role in exerting cell proliferation and inhibiting apoptosis.

MiR-215-5p promotes the proliferation of cells through the P53 signaling pathway

We found by Western blot experiments that the expression of MDM2 was 0.51 ± 0.04 in miR-215-5p overexpression, which was significantly higher than 0.30 ± 0.06 in the control group, P < 0.05; after inhibition of miR-215-5p, the expression of MDM2 was 0.20 ± 0.04, which was significantly lower than 0.30 ± 0.06 in the control group, P < 0.05. For miR-215-5p overexpression, the expression of P53 was 0.20 ± 0.06, which was significantly lower than 0.31 ± 0.08 in the control group, P < 0.05; after inhibition of miR-215-5p, the expression of P53 was 0.53 ± 0.10, which was significantly higher than 0.31 ± 0.08 in the control group, P < 0.05. For miR-215-5p overexpression, the expression of p21 was 0.27 ± 0.03, which was significantly lower than 0.44 ± 0.05 in the control group, P < 0.05; after inhibition of miR-215-5p, the expression of p21 was 0.59 ± 0.10, which was significantly higher than 0.44 ± 0.05 in the control group, P < 0.05 (Figure 5I). The original figure is Figure 5F. These data results suggest that miR-215-5p can function through the MDM2-P53 signaling pathway.

MDM2 inhibitors can restore P53 signaling pathway activity and cell proliferation

By adding MDM2 inhibitor RG7388 to miR-215-5p mimics, we found that the protein expression of Caspase3 was 0.08 ± 0.01 after adding the inhibitor, which was significantly higher than 0.04 ± 0.01 in the mimics group, P < 0.05, but still decreased compared with 0.15 ± 0.02 in the control group, P < 0.05; the protein expression of P53 was 0.32 ± 0.04, which was significantly higher than 0.21 ± 0.04 in the mimics group, P < 0.05, but still decreased compared with 0.49 ± 0.06 in the control group, P < 0.05 (Figure 5J), and after adding the inhibitor group, the cell proliferation activity was 113.60 ± 3.00 (%), which was significantly lower than 124.10 ± 4.10 (%) in the mimics group, P < 0.05, but still increased compared with 100.00 ± 0.00 (%) in the control group, P < 0.05 (Figure 5K).The original figure is Figure 5E and Figure 5G. It was also shown to some extent that miR-215-5p exerts biological functions by targeting MDM2, which begins to return to normal when MDM2 inhibitors are added.

Discustion

In recent years, the study of the molecular pathology and pathogenesis of STS has made the treatment of STS gradually accurate. Despite improved understanding of the molecular mechanisms of LPS, the regulation-associated mir molecules at targeted therapeutic sites including MDM2 remain understudied and their molecular mechanisms need to be further explored. MiRNAs play a role in almost all biological pathways including cell proliferation, apoptosis and tumorigenesis. Disturbed expression of miRNAs is closely associated with tumor progression(25). It can even affect the proliferation, metastasis and responsiveness of tumors to treatment(29).

It has been found in previous studies that miR-215 plays a cancer-suppressive role in a variety of tumors.MiR-215 is lowly expressed in colorectal cancer (CRC), and low levels of miR-215 correlate with TNM stage, lymph node metastasis, and depth of invasion, and promote CRC cell invasion and metastasis (27).In vitro experiments confirmed that overexpression of miR-215 targeted inhibition of stearoyl-CoA desaturase (SCD) expression, targeting the EGFR ligand epithelial-regulatory protein and its transcriptional inducer HOXB9, significantly inhibited the proliferation, migration, and invasion of CRC cells in vitro (30).MiR-215 is up-regulated in multiple myeloma (MM), and low levels of miR-215-5p are associated with poor prognosis in MM patients, and overexpression of miR-215 can inhibit RUNX1 expression in MM cells, while inhibiting PI3K/AKT/mTOR pathway activation, inducing apoptosis in MM cells, arresting the cell cycle in G1 phase and inhibiting cell proliferation (31).MiR-215 expression is down-regulated in papillary thyroid carcinoma (PTC), and low levels of miR-215 are associated with lymph node metastasis of PTC, and overexpression of miR-215 inhibits PTC cell proliferation and metastasis by targeting ARFGEF1, and regulates epithelial-mesenchymal transition through AKT/GSK-3β/Snail signaling to inhibit PTC cell metastasis (32).MiR-215 is underexpressed in non-small cell lung cancer (NSCLC), overexpression of miR-215 can inhibit cell proliferation, migration and cell cloning, and conversely down-regulation of miR-215 expression can promote NSCLC cell proliferation, migration and clonality (33).MiR-215 is lowly expressed in diffuse large B-cell lymphoma (DLBCL), and inhibits DLBCL cell growth and induces apoptosis by targeting and regulating KDM1B (34).

In addition, miR-215 can also play a cancer-promoting role. MiR-215 can promote epithelial-mesenchymal transition and cell proliferation by targeting and regulating LEFTY2 expression in endometrial cancer (35). Inhibition of retinoblastoma 1 (RB1) by overexpression of miR-215 in high-grade gliomas promoted cell proliferation (36). MiR-215 expression is up-regulated in gastric cancer (GC) and is associated with the progression of tumor invasion and tumor lymph node metastasis (TNM) stages (37), and overexpression of miR-215 can promote GC cell line migration and invasion, possibly by inhibiting various pathways such as RB1 (38), FOXO1 (39), and RUNX1 (40).

In conclusion, we predicted by bioinformatics analysis that miR-215-5p is one of the key nodal miRNAs in LPS cells, and may be associated with poor long-term prognosis.We selected the LPS cell line SW-872 as the experimental platform and confirmed that miR-215-5p directly targets the 3 ' UTR of MDM2 by dual-luciferase reporter assay.Co-localization of miR-215-5p with MDM2 was confirmed by qRT-PCR and FISH, and overexpression of miR-215-5p could increase MDM2 expression, inhibit miR-215-5p expression but also inhibit MDM2 expression.We found by cell phenotype assay that overexpression of miR-215-5p could significantly promote the proliferation activity, increase the colony formation rate, inhibit apoptosis, promote cell cycle progression, and increase cell invasiveness of SW-872 cells, and conversely inhibition of miR-215-5p expression would significantly inhibit the proliferation activity, decrease the colony formation rate, induce apoptosis, intervene

in the G2 phase of the cell cycle, and reduce cell invasiveness of SW-872 cells.We found by WB that overexpression of mir-215-5p promoted the expression of PCNA and inhibition of mir-215-5p decreased the expression level of PCNA, while overexpression of mir-215-5p promoted the high expression of the inhibitory apoptotic factor Bcl-2, inhibited the expression levels of the apoptotic factors Bax and caspase-3, and inhibited mir-215-5p, playing the opposite result.Our further study found that mir-215-5p overexpression promoted the expression of MDM2 while inhibiting the protein expression levels of downstream P53 and p21.By adding the MDM2 inhibitor RG7388 to mir-215-5pmimics, we found that the protein expression of Caspase3 and P53 was increased and the cell proliferation activity was decreased, indicating to some extent that mir-215-5p exerts its biological function by targeting MDM2, and when the MDM2 inhibitor was added, the biological function began to return to normal.

Conclusion

In conclusion, our experiments show that overexpression of miR-215-5p can promote cell proliferation, inhibit apoptosis, promote cell invasion and metastasis by targeting the MDM2-P53 signaling pathway in LPS cells SW-872, and inhibit miR-215-5p can play an opposite role. This study reveals some mechanisms in the progression of LPS, and helps to further explore the molecular mechanism and clinical treatment of LPS in the future. Targeting the miR-215-5p-MDM2-P53 signaling pathway may be a potential molecular targeted therapeutic strategy for LPS.

Materials And Methods

Bioinformatic analysis

GEO database was used for the screening of differentially expressed mRNAs and miRNAs between LPS and normal control tissues, where mRNA data were derived from GSE21122 and miRNA data were derived from GSE36982. Screening was performed by GEO2R (Fig. https://www.ncbi.nlm.nih.gov/geo/geo2r/). The screening criteria for mRNA were | logFC | > 2, and bonferron corrected P < 0.05, and the screening criteria for miRNA were | logFC | > 1.5, and bonferron corrected P < 0.05. The selected differentially expressed genes were subjected to GO and KEGG functional enrichment analysis by applying STRING, and the screening criteria were taken as P < 0.05 after correction. MiRTarBase(41), miRWalk(42) and TargetScan(43) databases were applied to predict all regulated target genes of differentially expressed miRNAs. Only target genes that were predicted simultaneously in the three databases were included in the analysis. The mRNA-miRNA regulatory network was constructed by overlapping the target genes of differentially expressed miRNAs with the genes of differentially expressed mRNAs. STRING(44) was applied to construct a protein-protein interaction network, and Cytoscape was applied to fuse it with the mRNA-miRNA regulatory network, and the fusion network was topologically analyzed using the CytoHubba plugin to screen the top 10 key nodes. Survival analysis of miR-215-5p expression in the TCGA database with overall survival time for DDL was implemented by LinkedOmics(45). MiR-215-5p was predicted for it regulatory relationship with MDM2 using TargetScan(43).

Cell lines and culture

The human liposarcoma cell line SW-872 was purchased from the American Type Culture Collection (ATCC), and the cell line used in the validation experiment of short tandem repeat (STR) DNA profiling matched exactly with the SW-872 cell line. SW-872 cells were lysed and cultured in DMEM medium containing 10% fetal bovine serum at 37°C and 5% CO2. SW-872 cells were transferred into a centrifuge tube containing 5ml medium (DMEM + 15%

FBS + 1% (Penicillin-Streptomycin Solution)) at a ratio of 1:3, centrifuged to collect cells, suspended with complete medium containing 10% fetal bovine serum, inoculated into a culture dish, gently blown and mixed well, and cultured at 37℃ under 5% CO2 saturated humidity. When the cell density reached 80%, 1 ml 0.25% trypsin was added to digest and collect the cells, which were passaged in a ratio of 1:3, and the culture was expanded at 37 ° C with 5% CO2 saturated humidity.

QRT-PCR

MiR-215-5p and MDM2 fluorescent real-time quantitative PCR primers were designed by DNAMAN software（table 3） and synthesized by Shanghai Sangon Co. Ltd. 2 ul 5 × PrimeScript Buffer, 0.5 ul PrimeScript RT Enzyme Mix I, 0.5 ul Oligo (dT) 15 (15 μM), 0.5 ul Randommers (100 μM), Total RNA 500 ng, RNase Free dH2O were added to 10 ul, respectively, mixed well and briefly centrifuged, heated at 37 ° C for 15 min, 85 ° C for 5 s, and diluted to 35 μl on a PCR instrument to obtain reverse transcribed cDNA. QPCR reaction: Forward primer 10 μ M0.4 ul, 0.4 ul Reverse primer 10 μM, 2XSYBR Select Master Mix (2 ×) 10 ul, RNase-free water 4.8 ul, cDNA template 4 ul, 50 × ROX Reference Dye 20.4 μl, prepared into 20 ul system, mixed well, maintained on the instrument at 95℃, 10 min, 95℃, 15s, 60℃ 60s, 95℃, 15s, 40 cycles, melting curve 60℃ 1 min, 95℃ 15s, 1 cycle, so as to obtain qPCR reaction results, using 2-ΔΔCt method for result quantification calculation.Three biological replicates were performed for each group.

Dual luciferase reporter gene

MiR-215-5p or control was cotransfected with pYr-MirTarget-MDM2 3 ' UTR into cells according to the groups as indicated using lipofectamine 2000 as transfection reagent, and fluorescence intensity was measured after 48 hours in the presence of firefly luciferase as an internal reference.Three biological replicates were performed for each group.

cell phenotype experiments

The effect of miR-215-5p on cell proliferation activity was explored by MTT colorimetric assay: the above cells were cultured for 24 h, 48 h, and 72 h according to the groups, 10 μL MTT was added to each well and cultured at 37 ° C for 4 h. The culture medium was aspirated and shaken with 150 μL DMSO for 10 min, and the absorbance OD568 of each well was measured by a microplate reader.Three biological replicates were performed for each group.

Flow cytometry was used to investigate the effects of miR-215-5p on cell cycle and apoptosis: cells were taken according to groups, digested with 0.25% trypsin without EDTA, resuspended and washed and fixed in 70% ethanol at 4 ° C for more than 4 h. Ribonuclease (RNase) was added and bathed in water at 37 ° C for 30 min; propidium iodide (PI) working solution was stained in the dark at 4 ° C for 30 min and then detected by flow cytometry. At the same time, the cells were taken according to the groups, digested with 0.25% trypsin without EDTA, resuspended and washed and reacted using the AnnexinV-APC/7-AAD apoptosis detection kit according to the instructions, and detected on the flow cytometer.Three biological replicates were performed for each group.

Cell scratch and invasion assay

Use a marker pen behind the 6-hole plate, use a ruler to make comparison, and evenly draw a horizontal line to pass through the hole at interval of 0.5 cm. The treated cells were divided into groups, inoculated in a six-well

plate, and cultured at 37℃ and 5% CO2. When the cell density reached about 90%, a vertical scratch was made, and photographs were taken at 0h and 48h.Three biological replicates were performed for each group.

The treated cells were taken according to groups, washed, resuspended, counted and diluted, inoculated in the prepared Matrigel-transwell reaction system, and cultured in 5% CO2 at 37℃ for 24 hours; the cells were fixed in 70% ice-cold ethanol solution for 1 hour, stained with crystal violet and observed and photographed under a microscope.

Colony formation assay was performed to investigate the effect of miR-215-5p on colony formation: cells were diluted in suspension according to groups and seeded in 6-well plates at a density of 300 cells. Culture for 3 weeks. When clones appeared, they were counted after methanol fixation and stained with crystal violet. Colony formation rate = colony count/inoculated cell count 100%.Three biological replicates were performed for each group.

Detection of MDM2 Expression by Immunofluorescence Single Labeling

In the culture plate, the slides that had climbed the cells were immersed with PBS for 3 times, 3 min each time; the reptiles were fixed with 4% paraformaldehyde for 15 min, and the slides were immersed with PBS for 3 times, 3 min each time; 0.5% TritonX-100 (prepared with PBS) was permeabilized at room temperature for 20 min; the slides were immersed with PBS for 3 times, PBS was blotted with absorbent paper, normal goat serum was added to the slides, and blocked at room temperature for 30 min; the blocking solution was absorbed with absorbent paper, without washing, a sufficient amount of diluted primary antibody (1:100) was added to each slide and placed in a wet box, and incubated overnight at 4 ° C; the reptiles were immersed with PBST for 3 times, 3 min each time, and the excess liquid on the reptiles was blotted with absorbent paper followed by dripping of diluted fluorescent secondary antibody (1:100), and the sections were immersed with PBST for 3 times, 3 min each time. Three biological replicates were performed for each group.

Detection of miR-215-5p expression by FISH

Cell crawls were fixed in 4% paraformaldehyde (DEPC) for 20 min and washed three times by shaking on a destaining shaker in PBS (pH 7.4) for 5 min each. Gene strokes were circled, and proteinase K (20 ug/ml) was added dropwise for digestion for 6 min according to different index characteristics of different tissues. After rinsing with pure water, PBS was washed three times × 5 min. The prehybridization solution was dropped for 1 h in a 37 ° C incubator. The prehybridization solution was poured off, and the hybridization solution (containing probe miR215 at a concentration of 500 nM) was dropped and hybridized overnight at 42 ° C. The hybridization solution was washed off, 2 × SSC, 10 min at 37 ° C, 1 × SSC, 2 × 5 min at 37 ° C, and 10 min at 0.5 × SSC 37 °. If there are more non-specific hybridizations, formamide washing can be added, and the hybridization solution containing secondary standard probes can be dropped and incubated at a dilution ratio of 1:400.42 ° for 3 hours. The latter 2 × SSC, washed at 37 ° C for 10 min, 1 × SSC, washed at 37 ° C for 2 × 5 min, and 0.5 × SSC at 37 ° for 10 min. Drop blocking solution: Drop blocking serum at room temperature for 30 min. Gutta mouse anti-digoxigenin-labeled peroxidase (anti-DIG-HRP): The blocking solution was decanted and anti-DIG-HRP was added. Incubation was performed for 50 min at 37 ° C, followed by three × 5 min PBS washes. Dropping of CY3-TSA: add CY3-TSA reagent and allow to react at room temperature for 5 min, protected from light. After washing with PBS three times × 5 min. The sections were dropped with DAPI staining solution and incubated in the dark for 8 min, rinsed and then dropped with anti-fluorescence quenching mounting medium for mounting. Sections were

observed and images were collected under a Nikon upright fluorescence microscope, and DAPI-stained nuclei were blue with Cy3-labeled red light under UV excitation.Three biological replicates were performed for each group.

CCK8 reaction

RG7388 is an MDM2-specific inhibitor. RG7388 was added to SW-872 mimics, and after 48 hours of cell culture, 10 μl cck8 was added to each well and cultured at 37 ° C for 4 hours; the absorbance OD450 of each well was measured by a microplate reader.Three biological replicates were performed for each group.

WB was used to detect the expression changes of caspase-3, MDM2, P53, P21, PCNA, Bax, and Bcl-2

After cell lysis, centrifugation, and BCA quantification in different groups, the protein expression of caspase-3, MDM2, P53, P21, PCNA, Bax, and Bcl-2 was detected. METHODS: 5% stacking gel and 12% separation gel, sample denaturation and sample loading, electrophoresis and membrane transfer were prepared. The membrane was loaded into 5% TBST blocking solution, prepared and shaken at room temperature for 2 h. 5 ml primary antibody diluent was added and kept at 4 ° C overnight. 10 ml of secondary antibody (1:1000 dilution) was placed on a shaker for 2 h. Color was developed and developed by compression exposure in a dark room. Results BandScan was used to analyze the gray value of the film, and the ratio of the intensity of the detected protein band to that of the protein band (%) was calculated, respectively.Three biological replicates were performed for each group.

Statistical Analysis

In this study, SPSS 22.0 software was used for data processing. All data were expressed as mean ± standard deviation (x ± s). One-way analysis of variance was performed for measurement data. LDS method was used for pairwise comparison. The test level $\alpha = 0.05$, $P < 0.05$ was considered statistically significant, and $P < 0.01$ was considered very significant.

Declarations

Ethics and consent to participate

Not applicable.

Consent for publication

Not applicable.

Availability of data and materials

The relevant data supporting the conclusions of this article are included within the article and its additional files.

Competing interest

The authors do not have any possible conflicts of interest.

Funding

The authors would like to thank the National Natural Science Foundation of China Project (81360282), the Natural Science Foundation of Science and Technology Department of Xinjiang Urumqi Autonomous Region (2015211C114), the Science and Technology Bureau of Urumqi Project (Y 141310040), and the Postgraduate Innovation Project of Xinjiang Urumqi Autonomous Region (XJ2021G227) for their financial support of this study.

Author Contributions

This study was designed by Zhengnan Song and Jingping Bai, and the experimental method was given by Zhengnan Song and Renbing Jiang. All experiments were done by Zhengnan Song, Junshen Wu, Wenpeng Yang, Junshen Wu. Wenpeng Yang participated in completing the data collection and data analysis. Zhengnan Song completed writing and revising the paper.

Acknowledgments

This study was done with the support of Xinjiang Tumor Hospital.

References

1. Gamboa, A. C., Gronchi, A., & Cardona, K. (2020). Soft-tissue sarcoma in adults: An update on the current state of histiotype-specific management in an era of personalized medicine. CA: a cancer journal for clinicians, 70(3), 200–229.
2. Siegel, R. L., Miller, K. D., & Jemal, A. (2018). Cancer statistics, 2018. CA: a cancer journal for clinicians, 68(1), 7–30.
3. Siegel, R. L., Miller, K. D., & Jemal, A. (2019). Cancer statistics, 2019. CA: a cancer journal for clinicians, 69(1), 7–34.
4. Casali, P. G., Abecassis, N., Aro, H. T., Bauer, S., Biagini, R., Bielack, S., Bonvalot, S., Boukovinas, I., Bovee, J., Brodowicz, T., Broto, J. M., Buonadonna, A., De Álava, E., Dei Tos, A. P., Del Muro, X. G., Dileo, P., Eriksson, M., Fedenko, A., Ferraresi, V., Ferrari, A., … ESMO Guidelines Committee and EURACAN (2018). Soft tissue and visceral sarcomas: ESMO-EURACAN Clinical Practice Guidelines for diagnosis, treatment and follow-up. Annals of oncology: official journal of the European Society for Medical Oncology, 29(Suppl 4), iv268–iv269.
5. Bock, S., Hoffmann, D. G., Jiang, Y., Chen, H., & Il'yasova, D. (2020). Increasing Incidence of Liposarcoma: A Population-Based Study of National Surveillance Databases, 2001–2016. International journal of environmental research and public health, 17(8), 2710.
6. Italiano A. (2018). Is There Value in Molecular Profiling of Soft-Tissue Sarcoma?. Current treatment options in oncology, 19(12), 78.
7. Vos, M., Koseła-Paterczyk, H., Rutkowski, P., van Leenders, G., Normantowicz, M., Lecyk, A., Sleijfer, S., Verhoef, C., & Grünhagen, D. J. (2018). Differences in recurrence and survival of extremity liposarcoma subtypes. European journal of surgical oncology: the journal of the European Society of Surgical Oncology and the British Association of Surgical Oncology, 44(9), 1391–1397.
8. Casadei, L., & Pollock, R. E. (2020). Extracellular vesicle cross-talk in the liposarcoma microenvironment. Cancer letters, 487, 27–33.
9. Tyler, R., Wanigasooriya, K., Taniere, P., Almond, M., Ford, S., Desai, A., & Beggs, A. (2020). A review of retroperitoneal liposarcoma genomics. Cancer treatment reviews, 86, 102013.

10. Tyler, R., Wanigasooriya, K., Taniere, P., Almond, M., Ford, S., Desai, A., & Beggs, A. (2020). A review of retroperitoneal liposarcoma genomics. Cancer treatment reviews, 86, 102013.
11. Ricciotti, R. W., Baraff, A. J., Jour, G., Kyriss, M., Wu, Y., Liu, Y., Li, S. C., Hoch, B., & Liu, Y. J. (2017). High amplification levels of MDM2 and CDK4 correlate with poor outcome in patients with dedifferentiated liposarcoma: A cytogenomic microarray analysis of 47 cases. Cancer genetics, 218–219, 69–80.
12. Setsu, N., Miyake, M., Wakai, S., Nakatani, F., Kobayashi, E., Chuman, H., Hiraoka, N., Kawai, A., & Yoshida, A. (2016). Primary Retroperitoneal Myxoid Liposarcomas. The American journal of surgical pathology, 40(9), 1286–1290.
13. Nguyen, D., Liao, W., Zeng, S. X., & Lu, H. (2017). Reviving the guardian of the genome: Small molecule activators of p53. Pharmacology & therapeutics, 178, 92–108.
14. Merkel, O., Taylor, N., Prutsch, N., Staber, P. B., Moriggl, R., Turner, S. D., & Kenner, L. (2017). When the guardian sleeps: Reactivation of the p53 pathway in cancer. Mutation research. Reviews in mutation research, 773, 1–13.
15. Binayke, A., Mishra, S., Suman, P., Das, S., & Chander, H. (2019). Awakening the "guardian of genome": reactivation of mutant p53. Cancer chemotherapy and pharmacology, 83(1), 1–15.
16. Ou, W. B., Zhu, J., Eilers, G., Li, X., Kuang, Y., Liu, L., Mariño-Enríquez, A., Yan, Z., Li, H., Meng, F., Zhou, H., Sheng, Q., & Fletcher, J. A. (2015). HDACi inhibits liposarcoma via targeting of the MDM2-p53 signaling axis and PTEN, irrespective of p53 mutational status. Oncotarget, 6(12), 10510–10520.
17. Das S. (2019). MDM2 Inhibition in a Subset of Sarcoma Cell Lines Increases Susceptibility to Radiation Therapy by Inducing Senescence in the Polyploid Cells. Advances in radiation oncology, 5(2), 250–259.
18. Chen, Q., Sun, X., Luo, X., Wang, J., Hu, J., & Feng, Y. (2020). PIK3R3 inhibits cell senescence through p53/p21 signaling. Cell death & disease, 11(9), 798.
19. Lee, J., Kim, J., Kim, E. M., Kim, U., Kang, A. R., Park, J. K., & Um, H. D. (2021). p21WAF1/CIP1 promotes p53 protein degradation by facilitating p53-Wip1 and p53-Mdm2 interaction. Biochemical and biophysical research communications, 543, 23–28.
20. Das S. (2019). MDM2 Inhibition in a Subset of Sarcoma Cell Lines Increases Susceptibility to Radiation Therapy by Inducing Senescence in the Polyploid Cells. Advances in radiation oncology, 5(2), 250–259.
21. de Jonge, M., de Weger, V. A., Dickson, M. A., Langenberg, M., Le Cesne, A., Wagner, A. J., Hsu, K., Zheng, W., Macé, S., Tuffal, G., Thomas, K., & Schellens, J. H. (2017). A phase I study of SAR405838, a novel human double minute 2 (HDM2) antagonist, in patients with solid tumours. European journal of cancer (Oxford, England: 1990), 76, 144–151.
22. Laroche-Clary, A., Chaire, V., Algeo, M. P., Derieppe, M. A., Loarer, F. L., & Italiano, A. (2017). Combined targeting of MDM2 and CDK4 is synergistic in dedifferentiated liposarcomas. Journal of hematology & oncology, 10(1), 123.
23. Han, X., Huang, T., & Han, J. (2020). Long noncoding RNA VPS9D1-AS1 augments the malignant phenotype of non-small cell lung cancer by sponging microRNA-532-3p and thereby enhancing HMGA2 expression. Aging, 12(1), 370–386.
24. Xiao, M., Li, J., Li, W., Wang, Y., Wu, F., Xi, Y., Zhang, L., Ding, C., Luo, H., Li, Y., Peng, L., Zhao, L., Peng, S., Xiao, Y., Dong, S., Cao, J., & Yu, W. (2017). MicroRNAs activate gene transcription epigenetically as an enhancer trigger. RNA biology, 14(10), 1326–1334.

25. Zhang, L., Yao, L., Zhou, W., Tian, J., Ruan, B., Lu, Z., Deng, Y., Li, Q., Zeng, Z., Yang, D., Shang, R., Xu, M., Zhang, M., Cheng, D., Yang, Y., Ding, Q., & Yu, H. (2021). miR-497 defect contributes to gastric cancer tumorigenesis and progression via regulating CDC42/ITGB1/FAK/PXN/AKT signaling. Molecular therapy. Nucleic acids, 25, 567–577.
26. Vos, P. D., Leedman, P. J., Filipovska, A., & Rackham, O. (2019). Modulation of miRNA function by natural and synthetic RNA-binding proteins in cancer. Cellular and molecular life sciences: CMLS, 76(19), 3745–3752.
27. Yan, J., Wei, R., Li, H., Dou, Y., & Wang, J. (2020). miR-452-5p and miR-215-5p expression levels in colorectal cancer tissues and their relationship with clinicopathological features. Oncology letters, 20(3), 2955–2961.
28. Wu, R. J., Zou, Y., Ma, X. D., & Zheng, R. J. (2020). Zhongguo shi yan xue ye xue za zhi, 28(5), 1570–1577.
29. Moradimotlagh, A., Arefian, E., Rezazadeh Valojerdi, R., Ghaemi, S., Jamshidi Adegani, F., & Soleimani, M. (2020). MicroRNA-129 Inhibits Glioma Cell Growth by Targeting CDK4, CDK6, and MDM2. Molecular therapy. Nucleic acids, 19, 759–764.
30. Xu, X., Ding, Y., Yao, J., Wei, Z., Jin, H., Chen, C., Feng, J., & Ying, R. (2020). miR-215 Inhibits Colorectal Cancer Cell Migration and Invasion via Targeting Stearoyl-CoA Desaturase. Computational and mathematical methods in medicine, 2020, 5807836.
31. Vychytilova-Faltejskova, P., Merhautova, J., Machackova, T., Gutierrez-Garcia, I., Garcia-Solano, J., Radova, L., Brchnelova, D., Slaba, K., Svoboda, M., Halamkova, J., Demlova, R., Kiss, I., Vyzula, R., Conesa-Zamora, P., & Slaby, O. (2017). MiR-215-5p is a tumor suppressor in colorectal cancer targeting EGFR ligand epiregulin and its transcriptional inducer HOXB9. Oncogenesis, 6(11), 399.
32. Liu, S., Zhang, Y., Huang, C., & Lin, S. (2020). miR-215-5p is an anticancer gene in multiple myeloma by targeting RUNX1 and deactivating the PI3K/AKT/mTOR pathway. Journal of cellular biochemistry, 121(2), 1475–1490.
33. β/Snail signaling by targeting ARFGEF1. Cell death & disease, 10(3), 195.
34. Cai, X., Peng, D., Wei, H., Yang, X., Huang, Q., Lin, Z., Xu, W., Qian, M., Yang, C., Liu, T., Yan, W., & Zhao, J. (2017). miR-215 suppresses proliferation and migration of non-small cell lung cancer cells. Oncology letters, 13(4), 2349–2353.
35. Gao, X., Cai, Y., & An, R. (2018). miR215 promotes epithelial to mesenchymal transition and proliferation by regulating LEFTY2 in endometrial cancer. International journal of molecular medicine, 42(3), 1229–1236.
36. Wu, R. J., Zou, Y., Ma, X. D., & Zheng, R. J. (2020). Zhongguo shi yan xue ye xue za zhi, 28(5), 1570–1577.
37. Meng, X., & Shi, B. (2017). miR-215 functions as an oncogene in high-grade glioma by regulating retinoblastoma 1. Biotechnology letters, 39(9), 1351–1358.
38. Chen, Z., Liu, K., Li, L., Chen, Y., & Du, S. (2017). miR-215 promotes cell migration and invasion of gastric cancer by targeting Retinoblastoma tumor suppressor gene 1. Pathology, research and practice, 213(8), 889–894.
39. Zang, Y., Wang, T., Pan, J., & Gao, F. (2017). miR-215 promotes cell migration and invasion of gastric cancer cell lines by targeting FOXO1. Neoplasma, 64(4), 579–587.
40. Li, N., Zhang, Q. Y., Zou, J. L., Li, Z. W., Tian, T. T., Dong, B., Liu, X. J., Ge, S., Zhu, Y., Gao, J., & Shen, L. (2016). miR-215 promotes malignant progression of gastric cancer by targeting RUNX1. Oncotarget, 7(4), 4817–4828.
41. Chou, C. H., Shrestha, S., Yang, C. D., Chang, N. W., Lin, Y. L., Liao, K. W., Huang, W. C., Sun, T. H., Tu, S. J., Lee, W. H., Chiew, M. Y., Tai, C. S., Wei, T. Y., Tsai, T. R., Huang, H. T., Wang, C. Y., Wu, H. Y., Ho, S. Y., Chen, P. R.,

Chuang, C. H., … Huang, H. D. (2018). miRTarBase update 2018: a resource for experimentally validated microRNA-target interactions. Nucleic acids research, 46(D1), D296–D302.

42. Sticht, C., De La Torre, C., Parveen, A., & Gretz, N. (2018). miRWalk: An online resource for prediction of microRNA binding sites. PloS one, 13(10), e0206239.
43. Agarwal, V., Bell, G. W., Nam, J. W., & Bartel, D. P. (2015). Predicting effective microRNA target sites in mammalian mRNAs. eLife, 4, e05005. https://doi.org/10.7554/eLife.05005
44. Szklarczyk, D., Gable, A. L., Lyon, D., Junge, A., Wyder, S., Huerta-Cepas, J., Simonovic, M., Doncheva, N. T., Morris, J. H., Bork, P., Jensen, L. J., & Mering, C. V. (2019). STRING v11: protein-protein association networks with increased coverage, supporting functional discovery in genome-wide experimental datasets. Nucleic acids research, 47(D1), D607–D613.
45. Vasaikar, S. V., Straub, P., Wang, J., & Zhang, B. (2018). LinkedOmics: analyzing multi-omics data within and across 32 cancer types. Nucleic acids research, 46(D1), D956–D963.

Tables

Table 1
Top 10 key nodes in network

Rank	Name	Score
1	CDKN2A	75
2	MYC	66
3	PPARG	60
3	SNAI2	60
5	CAV1	56
6	ID1	38
7	MiR-215-5p	36
8	RACGAP1	31
9	DTL	30
9	SMC4	30

Table 2
Targetscan prediction results

Seed of miR-215-5P		Site Type	Contex + + Score
Position 4592–4598 of MDM2 3' UTR	5' …CUCCCUGUCUUCUCUUAGGUCAC…	poorly conserved 7-mer-m8	-0.08
	| | | | |		
miR-215-5p	3' CAGACAGUUAAGUAUCCAGUA		

Table 3
PCR primer sequences

Gene	Primer	Sequence (5'-3')	PCR Products
U6	Forward	CGCTTCGGCAGCACATATAC	
	Reverse	AAATATGGAACGCTTCACGA	
Homo GAPDH	Forward	TCAAGAAGGTGGTGAAGCAGG	115bp
	Reverse	TCAAAGGTGGAGGAGTGGGT	
Homo MDM2	Forward	AGCAGGAATCATCGGACTCA	219bp
	Reverse	TGTGGCGTTTTCTTTGTCGT	
miR-215-5p	loop primer	GTCGTATCCAGTGCAGGGTCCGAGGTATTCGCACTGGATACGACGTCTGTCA	
	F primer	TGCGCATGACCTATGAATTGA	

Figures

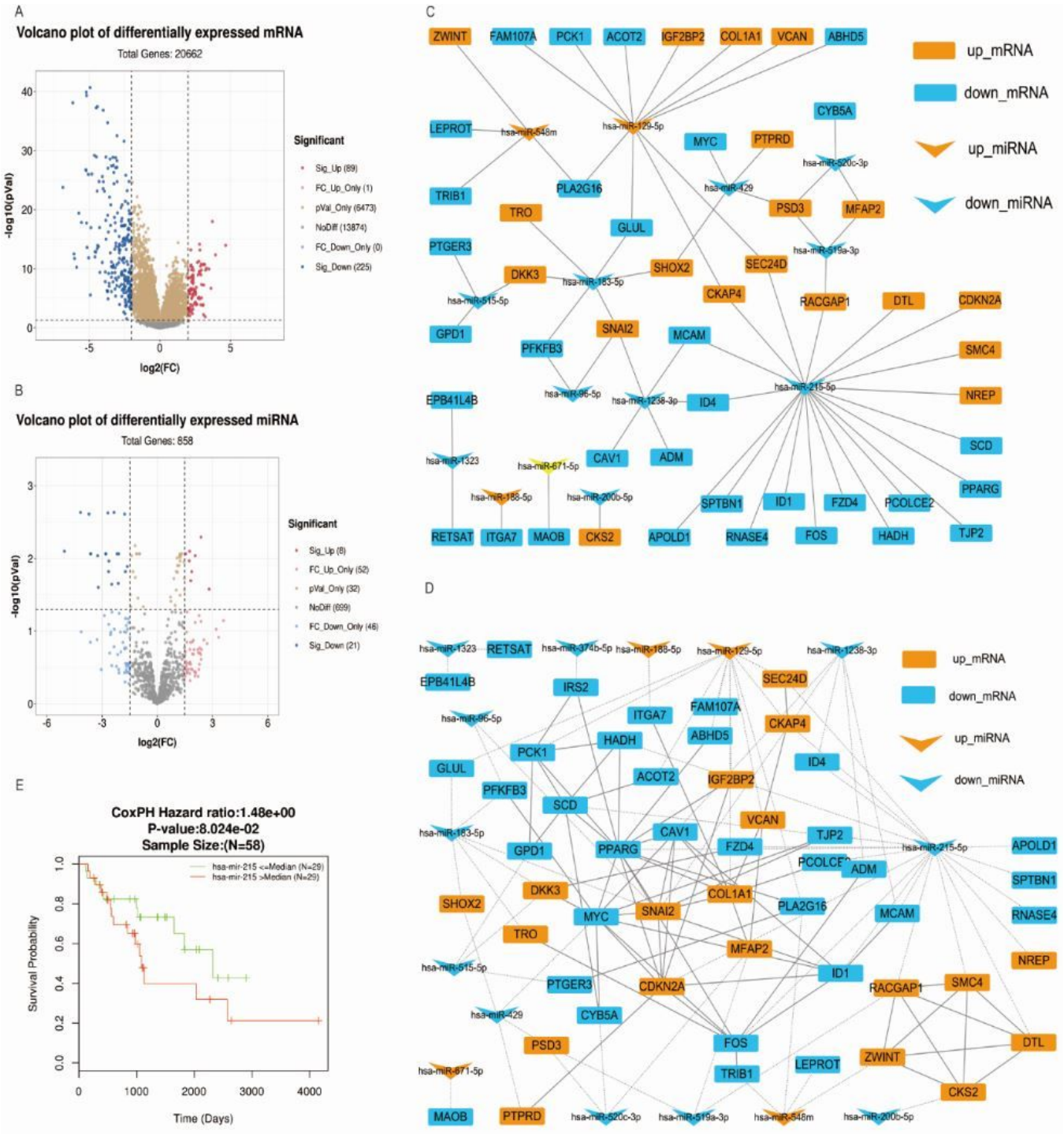

Figure 1

MiRNA and gene selection.

A and B screened differentially expressed mRNAs (A) and miRNAs (B) between LPS tissues and normal tissues; C showed the experimentally confirmed regulatory relationship between these mRNAs and miRNAs; D showed the miRNA-mRNA regulation and protein interaction fusion network, in which miR215-5p was in the central regulatory position; E was the survival analysis of the high and low miR-215-5p expression groups in LPS of TCGA.

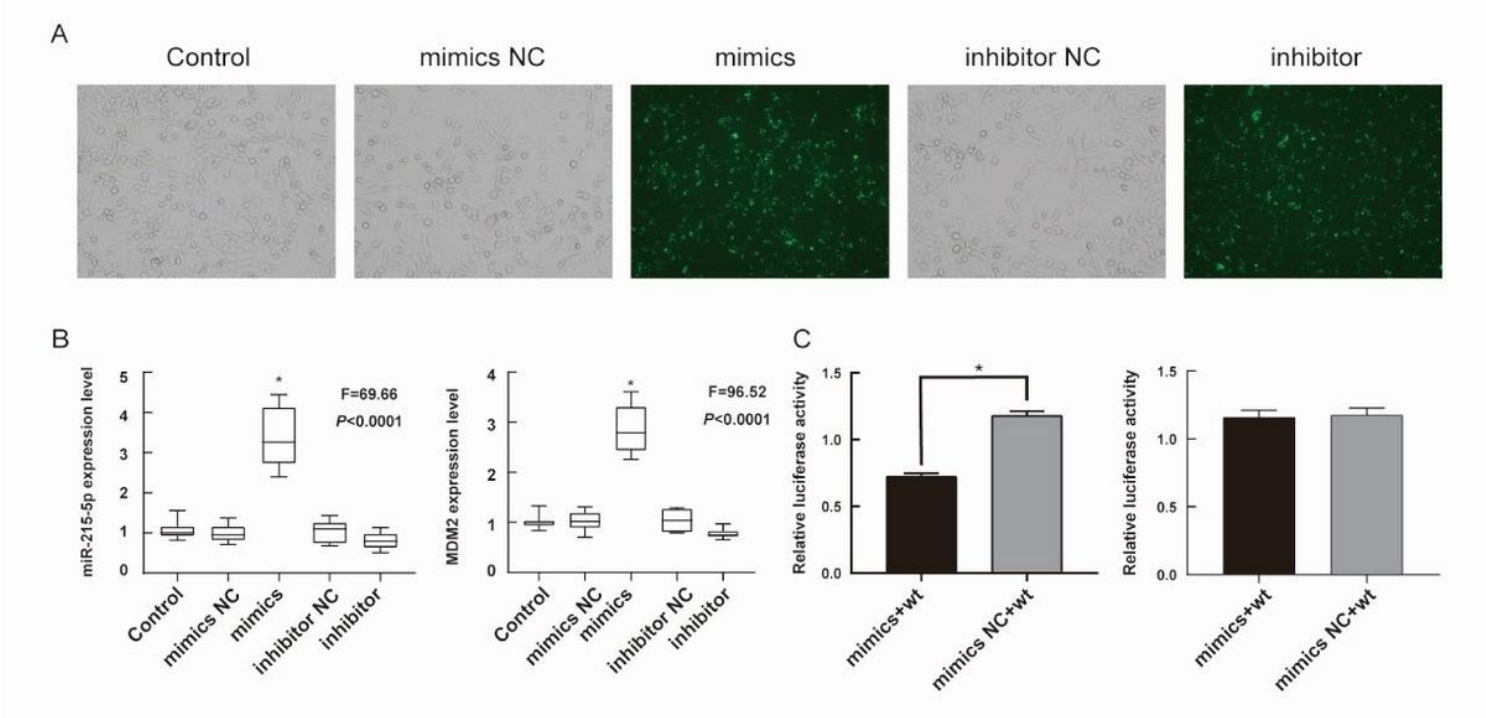

Figure 2

MiR-215-5P directly promotes MDM2 expression in LPS cells.

A shows that after miR-215-5p mimcs and miR-215-5p inhibitor transfection of cells, green fluorescence appeared; B indicates that the expression of miR-215-5p and MDM2 was significantly increased in the mimics group compared with the control group; C indicates that co-transfer of miR-215-5p-mimics + wt plasmid resulted in a decrease in the ratio of fluorescence intensity compared with the control group, with no significant difference between the other groups. * P < 0.05.

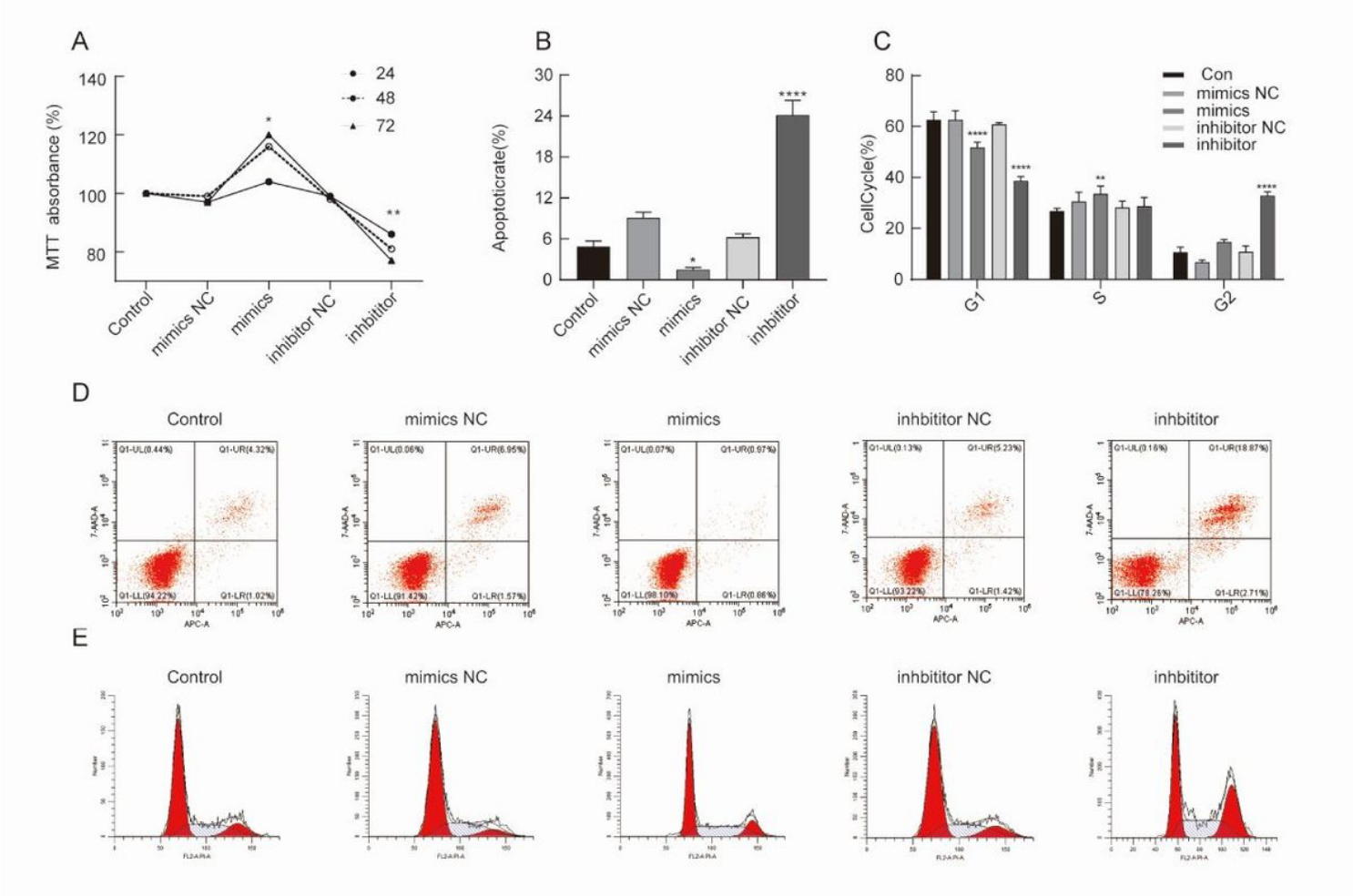

Figure 3

MIR-215-5p promotes proliferation and inhibits apoptosis in LPS cells.

A indicates that the cell proliferation rate in the miR-215-5p mimics group was significantly increased compared with the control group;B indicates that the apoptosis rate of the mimics group was significantly decreased compared with the control group, and the apoptosis rate of the inhibitor group was significantly increased compared with the control group; C indicates the cell cycle of the mimics group was significantly decreased in G1 phase, significantly increased in S phase, and did not change significantly in G2 phase, and the inhibitor group was significantly decreased in G1 phase, not significantly different in S phase, and significantly increased in G2 phase compared with the control group;

D is the raw data plot of apoptosis detected by flow cytometry; E is the original figure of flow cytometric cycle.* $P < 0.05$, ** $P < 0.01$,**** $P < 0.001$.

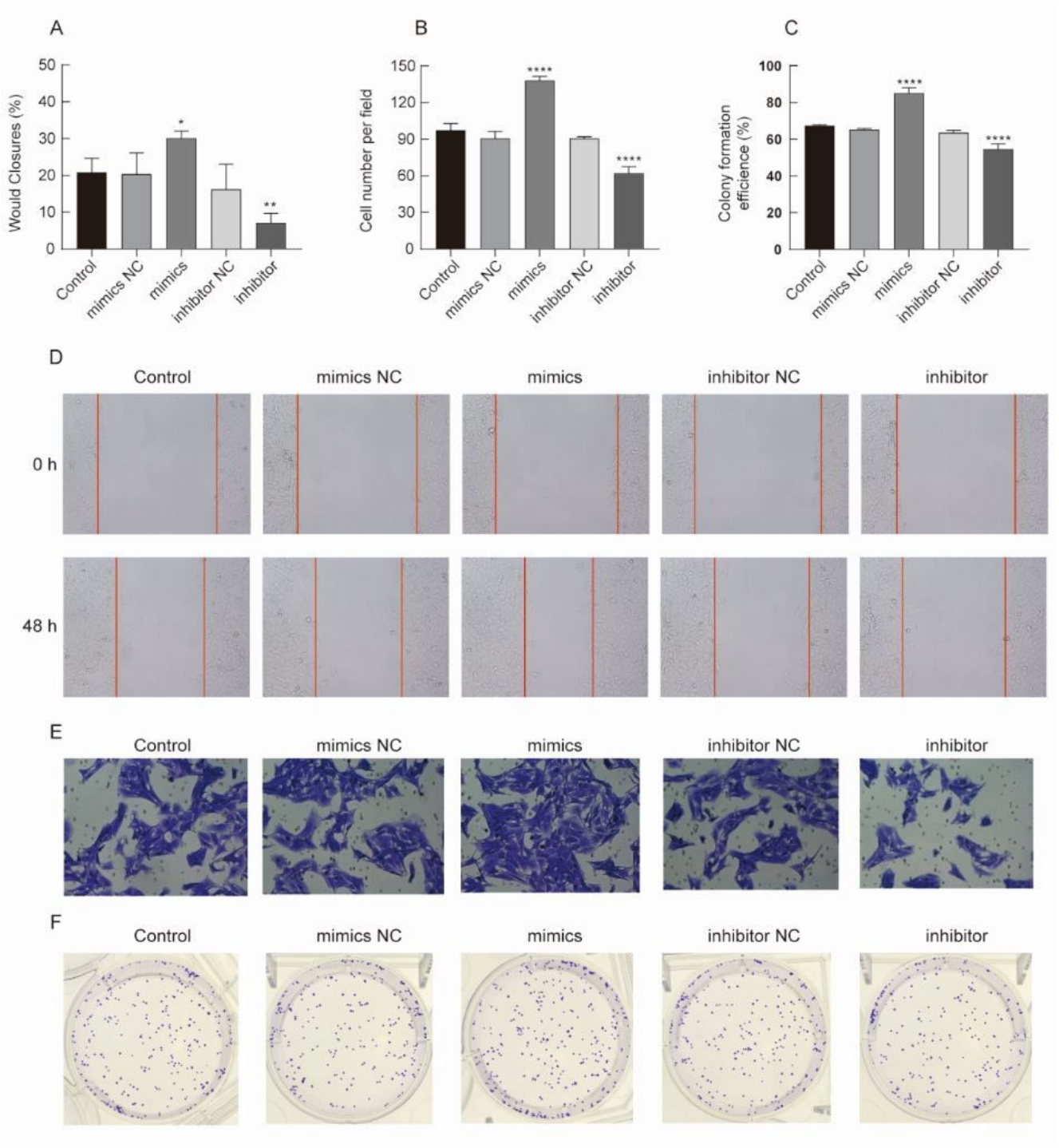

Figure 4

MIR-215-5p promotes invasion and metastasis in LPS cells.

A indicates that the cell healing area ratio was significantly increased in the mimics group and significantly decreased in the inhibitor group compared with the control group; B indicates that the number of cell invasion was significantly increased in the mimics group and significantly decreased in the inhibitor group compared with the control group;C indicates that the colony formation rate of the mimics group was significantly increased, and the colony formation of the inhibitor group was significantly decreased compared with the control group; D is the

original figure of cell healing assay; E is the original figure of cell invasion assay; and F is the original figure of cell colony formation assay.* P < 0.05, ** P < 0.01,**** P < 0.001.

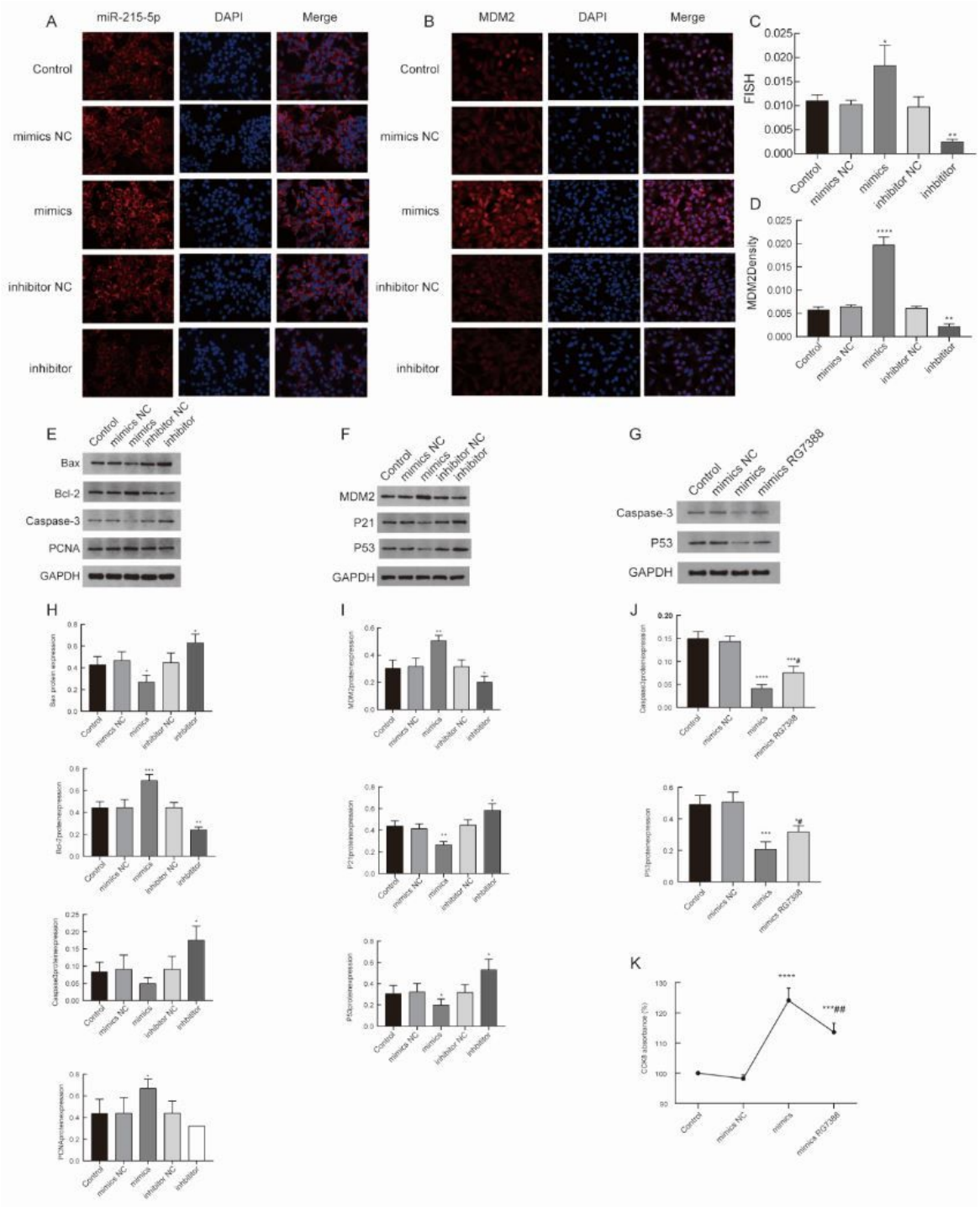

Figure 5

miR-215-5p Effects on Gene Expression.

A indicates that miR-215-5p co-localizes with MDM2; B represents MDM2 detected by immunofluorescence single labeling assay; C and D indicates that the expression of overexpressed MDM2 was significantly increased, and the expression of inhibited MDM2 was significantly decreased compared with the control group; E and F represent the original figures of the expression changes of caspase-3, MDM2, p53, p21, PCNA, bax, and bcl-2 detected by WB; G

indicates that miR-215-5p mimics were added with MDM2 inhibitor RG7388, the expression changes of Caspase3 and P53 were detected by WB;H indicates that compared with the control group, the expression of PCNA and Bcl-2 was significantly increased, the expression of Bax was significantly decreased, and the expression of caspase-3 was not statistically significant, while the expression of PCNA was not statistically significant, the expression of Bcl-2 was significantly decreased, and the expression of Bax and caspase-3 was significantly increased in the overexpression group; I indicates that the expression of MDM2 was significantly increased and the expression of P53 and p21 was significantly decreased in the overexpression group, while the expression of MDM2 was significantly decreased and the expression of P53 and p21 was significantly increased in the inhibition group, compared with the control group; J stated that by adding the MDM2 inhibitor RG7388 to mimic, the expression of caspase3 was significantly increased compared with mimic group, but still decreased compared with control group,and the expression of P53 was significantly increased compared with mimic group, but still decreased compared with control group; K indicates that the cell proliferation activity was significantly lower than that in the mimics group after the addition of inhibitors but still increased compared with the control group.

Supplementary Files

This is a list of supplementary files associated with this preprint. Click to download.

- Supplement1.doc